



Predicting evolution of ply cracks in composite laminates subjected to biaxial loading



John Montesano, Chandra Veer Singh*

Materials Science and Engineering, University of Toronto, 184 College St., Suite 140, Toronto, M5S 3E4, Canada

ARTICLE INFO

Article history:

Received 30 September 2014

Received in revised form

17 January 2015

Accepted 26 January 2015

Available online 4 February 2015

Keywords:

A. Laminates

B. Damage tolerance

C. Damage mechanics

C. Analytical modelling

C. Multiaxial loading

ABSTRACT

An energy-based model is developed to predict the evolution of sub-critical matrix crack density in symmetric multidirectional composite laminates for the case of multiaxial loading. A finite element-based numerical scheme is also developed to evaluate the critical strain energy release rate, G_{Ic} , associated with matrix micro-cracking, a parameter that previously required fitting with experimental data. Furthermore, the prediction scheme is improved to account for the statistical variation of G_{Ic} within the material volume by using a two-parameter Weibull distribution. The variation of G_{Ic} with increasing crack density is also accounted for based on reported experimental evidence. The simulated results for carbon/epoxy and glass/epoxy cross-ply laminates demonstrate the ability of the improved model to predict the evolution of multidirectional ply cracking. By integrating this damage evolution model with the synergistic damage mechanics approach for stiffness degradation, the stress-strain response of the studied laminates is predicted. Finally, biaxial stress envelopes for ply crack initiation and pre-determined stiffness degradation levels are predicted to serve as representative examples of stiffness-based design and failure criterion.

© 2015 Elsevier Ltd. All rights reserved.

1. Introduction

The emergence of polymeric composites as core materials for many different industrial applications has resulted in important studies aimed at predicting their long-term durability and damage tolerance capabilities. Particularly, the problem of transverse ply cracking in composite laminates has been investigated extensively during the last three decades [1–9]. Many of these studies have proposed models that are based on variational approaches [2,4], shear lag approximations [5], other stress-transfer methods [6], or explicitly on crack opening displacements [7]. However, most of the reported studies considered uniaxially loaded cross-ply laminates containing only 90° ply cracks, where a recent review on this subject was treated in Ref. [10]. This is mainly due to the limitations of some of the aforementioned models, which cannot account for variations in the laminate stacking sequence, or the scenario of simultaneous cracking in plies with different orientations. Practical applications require multidirectional laminates that

can provide more comprehensive directional stiffness properties, thus recent studies are increasingly focused on damage evolution and stiffness degradation of multidirectional laminates containing ply cracks in multiple orientations [11–22]. The models reported in these studies generally have the capability to consider cracking in multiple plies, but many cannot directly account for intra-ply crack interactions (i.e., the so-called crack shielding effect) or inter-ply crack interactions that result from the constraining effects between adjacent plies in a laminate. Due to the complex nature of the damage evolution process in multidirectional laminates, available experimental data has been mainly limited to uniaxial tensile loading, allowing corresponding crack evolution models to be calibrated and validated [13, 19]. The problem becomes more complex when multidirectional laminates are subjected to multiaxial loads, representing the real application of composite structures. In these situations, the evolving damage processes and the corresponding material behaviour will undoubtedly change [23]. For example, in addition to cracking in the 90° and off-axis plies, a biaxial stress state will cause axial splitting cracks to develop in the on-axis plies as has been experimentally observed [24]. Furthermore, the evolving multidirectional ply cracks initiate and progress differently, resulting in complex three dimensional stress states in the laminate that vary with

* Corresponding author. Tel.: +1 416 946 5211; fax: +1 416 978 4155.

E-mail addresses: john.montesano@utoronto.ca (J. Montesano), chandraveer.singh@utoronto.ca (C.V. Singh).

progressive loading. The development of an accurate physically-based analytical model that accounts for such complexities is essential for predicting the durability and damage tolerance capabilities of practical composite structures, which would enable safer and more cost effective designs.

In recent years, a number of reported studies have proposed damage evolution models for composite laminates that account for multiaxial loading [6,25–32], but these models have notable shortcomings that limit their applicability. On one hand, some use ultimate failure criteria to predict failure envelopes [25], while others use simplified strength-based approaches and may not consider the evolution of specific physical damage modes [26,28]. Due to the progressive nature of failure development in composites, it is important not only to consider damage evolution, but also to combine this with accurate stiffness predictions in a coherent fashion. Furthermore, many of these models are applicable only to laminates containing only cracks in one transverse direction [6, 27]. Additionally, some models simplify the inherent complex boundary value problem by assuming that a two dimensional geometric representation of ply cracks is sufficient [27, 28, 31]. Such a representation does not accurately capture the local crack behaviour and the surrounding stress state, and thus a three dimensional solution becomes necessary when multiple ply cracks are present [23]. A three dimensional model is necessary in order to accurately capture the constraining effect between the adjacent plies in a laminate. Due to inherent simplifications, the models cannot account for the interaction between cracks in different adjacent layers caused by the ply constraining effect [29, 30, 32], despite experimental observations to the contrary [13]. Another issue with existing models is that some do not consider the statistical variation of the crack evolution process [27–30], arising due to variations with manufacturing processes. Finally, all of the indicated models rely on extensive empirical data for calibration of the damage (or failure) parameters, often relying on fitting numerical constants to match experimental data. The predictive capabilities are therefore limited in scope and application.

The main objective of this study is to develop an approach for predicting damage evolution in multidirectional composite laminates subjected to multiaxial loading that accounts for stochasticity of the damage process. An energy-based approach for predicting crack density evolution developed by Joffe et al. [7] for cross-ply laminates, and later extended for multidirectional laminates by Singh and Talreja [19], is further improved here for the case of multiaxial loading. Improvements are also made to account for the stochastic nature of the cracking process, which is particularly important for an accurate prediction of crack initiation strain levels. The model capabilities are highlighted for a number of carbon fiber/epoxy and glass fiber/epoxy cross-ply laminates, and the predictions are verified with experimental data available in the literature. It should be noted that to the knowledge of the authors, experimental or predicted crack density evolution data for multiaxially loaded cross-ply laminates are not available in the literature; thus, a complete prediction of overall deformation behaviour of composites undergoing progressive damage under multiaxial loading has not been possible. This is resolved by integrating the energy-based damage evolution model with a synergistic damage mechanics model for predicting stiffness degradation. Such an approach combines the strengths of micromechanics and continuum mechanics, relying on computational micromechanics, in lieu of experimental testing, to calibrate the material damage parameters [18, 23]. Also, since the computational micromechanical models are three-dimensional, ply constraining effects and both intra-ply and inter-ply crack interactions are explicitly considered.

2. Modeling approach

2.1. Damage representation, stiffness degradation and laminate constitutive equations

Consider a general laminate consisting of on-axis, off-axis and transverse plies with unidirectional fibers as shown in Fig. 1. The evolution of ply cracks in multidirectional laminates subjected to

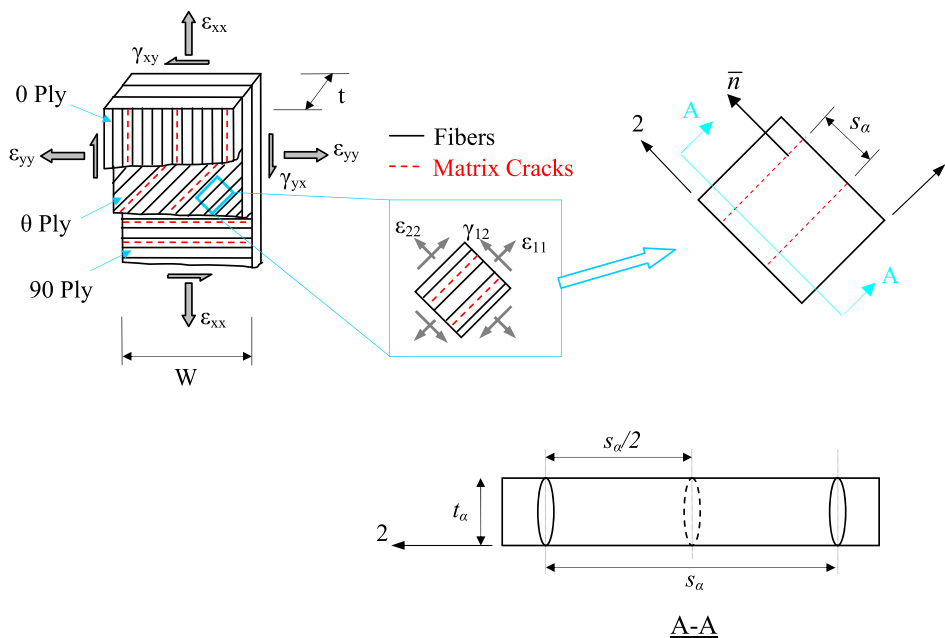


Fig. 1. A representative volume element of a damaged multidirectional laminate subjected to a 2D multi-axial strain state, with local transformed strain components and a virtual crack shown.

uniaxial tensile quasi-static loading has been reported in many studies [5, 13, 14, 19]. Matrix or ply cracks initiate and multiply in the transverse and off-axis plies, where a state of multiple matrix cracking ensues. These cracks have been observed to span the ply thickness, orienting themselves along the fiber direction (see Fig. 1). The multidirectional crack state becomes even more complex when the laminates are subjected to multiaxial strains, resulting in distinct crack evolution characteristics due to the altered local transformed strain components (see Fig. 1) [23]. Following continuum damage mechanics concepts, the damage state within the laminate volume can be described through a second-order tensor [33]. This tensor for damage mode, α , corresponding to ply cracking in a particular orientation is defined by

$$D_{ij}^{(\alpha)} = \frac{\kappa_\alpha t_\alpha^2}{s_\alpha t} n_i n_j \quad (1)$$

where t_α is the cracked ply thickness, s_α is the average crack spacing, n_i are components of the crack surface normal unit vector (see Fig. 1), and κ_α is a constraint parameter. Further details of this damage description can be found in Refs. [18, 23]. The damage tensor components presented in Eq. (1) are used in the constitutive equations to derive the stiffness tensor of the cracked. The stiffness tensor, C_{ijkl} , for a thin symmetric orthotropic laminate containing multidirectional damage is given by Ref. [23].

$$C_{ijkl} = \begin{bmatrix} \frac{E_x^o}{1 - \nu_{xy}^o \nu_{yx}^o} & \frac{\nu_{xy}^o E_y^o}{1 - \nu_{xy}^o \nu_{yx}^o} & 0 \\ \frac{\nu_{xy}^o E_y^o}{1 - \nu_{xy}^o \nu_{yx}^o} & \frac{E_y^o}{1 - \nu_{xy}^o \nu_{yx}^o} & 0 \\ 0 & 0 & G_{xy}^o \end{bmatrix} + \sum_{\alpha} a_\alpha D_\alpha \begin{bmatrix} 2a_1^{(\alpha)} & a_4^{(\alpha)} & 0 \\ a_4^{(\alpha)} & 2a_2^{(\alpha)} & 0 \\ 0 & 0 & 2a_3^{(\alpha)} \end{bmatrix} \quad (2)$$

corresponding damage-dependent linear elastic constitutive equations can be used to relate the stresses σ_{ij} and strains ϵ_{kl} as

$$\sigma_{ij} = C_{ijkl} \left(D_{ij}^{(\alpha)}(\rho) \right) \epsilon_{kl} \quad (3)$$

where ρ is the crack density. In previous versions of the synergistic damage mechanics model [21], $D_{ij}^{(\alpha)}$ were assumed to be independent of evolving crack density which resulted in over-prediction of stiffness degradation at high damage levels. This simplification was eliminated in a recent report [23].

2.2. Damage initiation and evolution

The damage evolution models available in the literature can be categorized as either (i) strength-based, where the lamina transverse strength is used to predict crack initiation, or (ii) energy-based, where fracture mechanics concepts are considered to account for the energetics of ply cracking. One major advantage of energy-based methods is that they can account for the variation of crack initiation strains with ply thickness [7], and is thus utilized here. The approach utilizes the concepts of Irwin's virtual crack closure technique [34], where the reader is referred to Ref. [19] for more details. Following experimental observations, it is assumed here that ply cracks initiate as full through-the-thickness brittle cracks, and thus the focus is on the multiplication of these cracks (i.e., increasing crack density). According to Irwin [34], the energy released by a brittle cracking event is equal to the work required to close an open crack. Consider the two cracks states with crack spacing denoted by s_α and $s_\alpha/2$ for an arbitrarily oriented ply in a laminate shown in Fig. 1. Upon increasing the applied load additional cracks may form, increasing the number of cracks from N to $2N$. The work required to close the new N cracks is derived as [19].

$$W_{2N \rightarrow N} = N \frac{1}{\sin \theta} t_\alpha^2 \frac{1}{E_2} \left[(\sigma_2^\alpha)^2 \{2\tilde{u}_n^\alpha(s_\alpha/2) - \tilde{u}_n^\alpha(s_\alpha)\} + (\sigma_{12}^\alpha)^2 \{2\tilde{u}_t^\alpha(s_\alpha/2) - \tilde{u}_t^\alpha(s_\alpha)\} \right] \quad (4)$$

The first term on the right side of Eq. (2) contains the undamaged material engineering constants, namely E_x^o , E_y^o , G_{xy}^o , ν_{xy}^o , ν_{yx}^o , whereas the second term accounts for the effects of damage in different plies (i.e., different damage modes α) on the material stiffness. The $a_i^{(\alpha)}$ terms are material constants that are evaluated numerically for a certain laminate class, and the D_α terms are functions of the crack opening displacements (CODs) which can also be computed numerically using 3D finite element (FE) micromechanics (see Ref. [23]). Thus, for a given damage state, the

where E_2 is the transverse modulus, σ_2^α is the transformed ply level stress acting normal to the crack plane, and σ_{12}^α is the ply level shear stress of the undamaged ply. The normalized average crack opening displacement (COD) and crack sliding displacement (CSD) are denoted by \tilde{u}_n^α and \tilde{u}_t^α , respectively, and are associated with the varying crack density through an inverse sigmoidal function as detailed in Ref. [23]. The work terms in Eq. (4) representing mode I and mode II cracking can be written as

$$W_I = \frac{(\sigma_2^\alpha)^2 t_\alpha}{E_2} [2\tilde{u}_n^\alpha(s_\alpha/2) - \tilde{u}_n^\alpha(s_\alpha)], \quad W_{II} = \frac{(\sigma_{12}^\alpha)^2 t_\alpha}{E_2} [2\tilde{u}_t^\alpha(s_\alpha/2) - \tilde{u}_t^\alpha(s_\alpha)] \quad (5)$$

For a given loading condition, a criterion for crack multiplication can now be defined for general off-axis plies. A suitable mixed-mode criterion is defined as

$$\left(\frac{W_I}{G_{Ic}}\right)^a + \left(\frac{W_{II}}{G_{IIc}}\right)^b \geq 1 \tag{6}$$

where a and b are chosen constants [19]. The critical strain energy release rates associated with mode I (i.e., COD) and mode II (i.e., CSD) are denoted by G_{Ic} and G_{IIc} , respectively. It is important to note that these parameters are not material parameters in the sense of linear elastic fracture mechanics, but can be viewed as energy thresholds required for ply cracks to multiply, and are dependent on the particular laminate considered [19]. For cross-ply laminates that are not subjected to in-plane shear loading, the CSD for all plies can be ignored and the criterion is reduced to:

$$\frac{W_I}{G_{Ic}} \geq 1 \tag{7}$$

In order to utilize the criterion defined by Eq. (7), G_{Ic} must be determined for the considered laminate.

In previous work [19], G_{Ic} was calibrated by fitting the model to experimental crack density vs. applied strain data for a chosen reference laminate. In this study, the evaluation of G_{Ic} is accomplished through a numerical approach based on a modified crack tip closure technique [36–38]. Instead of modeling the crack tip, a through-the-thickness ply crack for the specific ply of interest is analyzed using 3D micromechanical FE analysis, which accurately captures the constraining effects between adjacent plies [23]. Thus the main difference between this approach and the previously established crack closure procedure is that the focus here is on crack multiplication and not on a single crack’s progression. For schematic purposes, consider the cross-ply laminate loaded in the direction normal to the 90° ply crack plane as shown in Fig. 2a. In order to represent crack initiation conditions, the crack spacing is assumed to be large ($= 100t_\alpha$) such that s_α approaches infinity [39]. The numerical procedure requires two separate analyses utilizing the same micromechanical FE model. The first analysis is conducted whereby springs with very large stiffness values are connecting all coinciding nodes on the crack surfaces, which allows for extraction of the total spring forces normal to the crack surface, $\sum F_n^i$. The second analysis consists of the same FE model without any springs as shown in Fig. 2a, which leads to the evaluation of the averaged COD, \bar{u}_n^α , for the given crack spacing. For both FE analyses, the uniaxial strain applied to the laminate model is equal to the crack initiation strain for that specific ply, which can be defined from experimental uniaxial stress–strain data (e.g., Refs. [5, 13]). The

benefit here is that the entire experimental crack density profile is not required, and the need for an iterative procedure to define G_{Ic} is eliminated [19]. The critical strain energy release rate is therefore determined by:

$$G_{Ic} = \frac{1}{2t_\alpha W} \left(\sum_i F_n^i \right) \bar{u}_n^\alpha \tag{8}$$

where W is the width of the FE model, which is arbitrary. A similar analysis can be conducted for the outer 0° plies of the cross-ply laminate in order to evaluate their corresponding G_{Ic} , which may in fact exhibit different G_{Ic} values since they are only constrained on one side. Note that this analysis corresponds to a reference uniaxial loading case for a laminate, whereby the evaluated G_{Ic} values are used for general multiaxial cases. Also note that if a reference uniaxial loading case cannot be analyzed for a particular laminate, a reference laminate can also be chosen to evaluate G_{Ic} [19].

Previous experimental studies have shown that the ply crack critical strain energy release rate, or the resistance to ply crack multiplication, tends to increase with increasing ply crack density, reaching a state of saturation at higher crack densities [5, 31, 35], (see plotted curve in Fig. 2b). This is a result of interacting stress fields between the cracks as more cracks appear, which is an experimentally observed phenomenon known as crack shielding. In order to define the variation of G_{Ic} , an analytical expression used by Zhang et al. [5] is adopted, and is define by

$$G_{Ic} = G_{Ic0} + G_{Icr}(1 - \exp(-r\rho_\alpha)) \tag{9}$$

where G_{Ic0} is initial critical strain energy release rate, and is evaluated numerically using Eq. (8). For the cross-ply laminates analyzed in this study, the scaling constant is found to be $G_{Icr} = 0.8 G_{Ic0}$, while the shape factor r is 1.5 and 15 for CFRP and GFRP laminates, respectively. Note that the crack density, ρ_α , is equal to the inverse of the crack spacing, s_α .

Another aspect that was missing from the previous model [19] is the stochastic nature of the ply crack multiplication process, which results from a random distribution of manufacturing flaws, local fiber fractions, or weakened fiber matrix interfaces [40–42]. Cracks tend to nucleate at the weakest regions in the laminate. The variation in crack resistance within the laminate volume is accounted for by a two-parameter Weibull distribution as:

$$G_{Ic0} = G_o \left[\ln \left(\frac{1}{1-F} \right) \right]^{\frac{1}{m}} \tag{10}$$

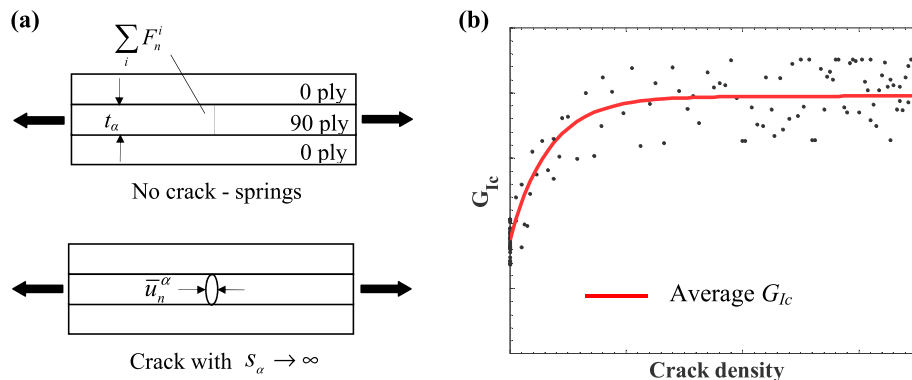


Fig. 2. (a) Schematic of numerical approach to evaluate the initial critical strain energy release rate, G_{Ic0} , for a cracked ply, (b) schematic of G_{Ic} values plotted against crack density.

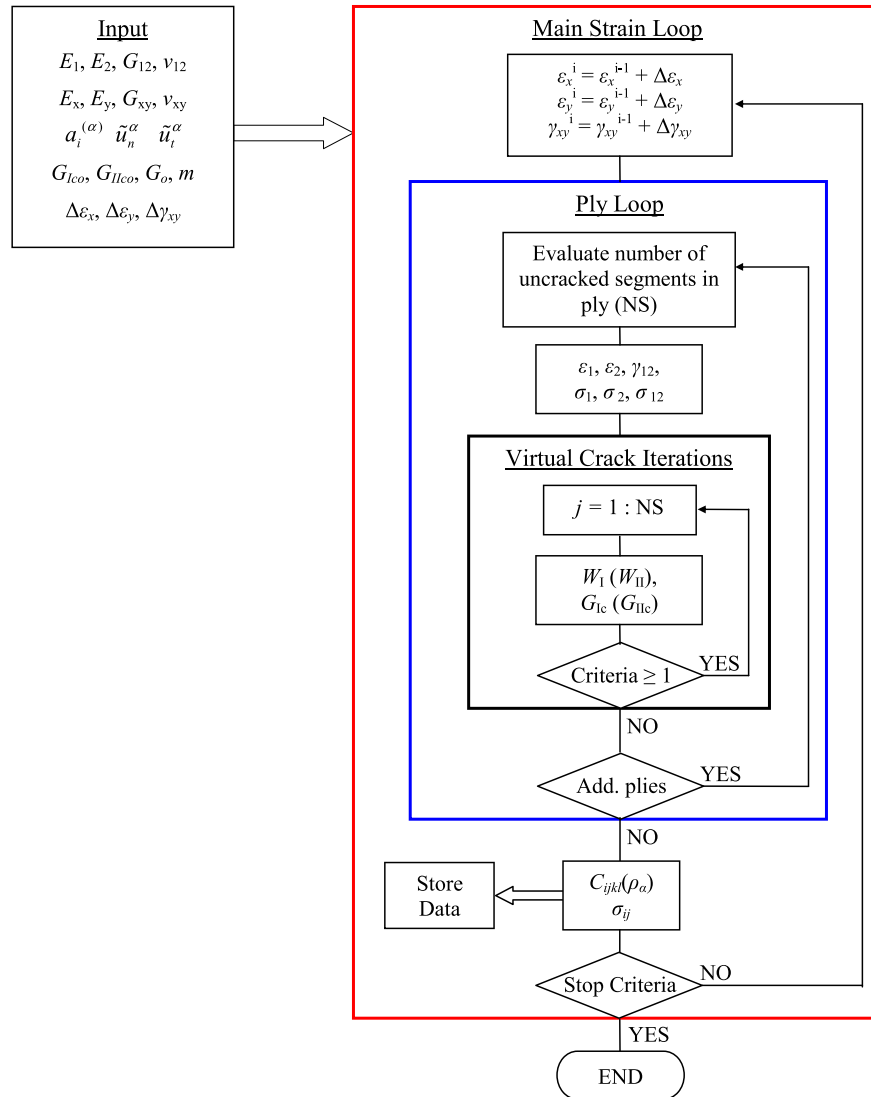


Fig. 3. General procedure for predicting ply crack evolution for general symmetric laminates using the developed model based on virtual crack closure technique.

where G_0 and m are the Weibull distribution parameters, and F is a random number in the interval $[0,1]$. The two Weibull parameters are evaluated from the mean and variance of G_{Ico} , as is described in Ref. [41]. In this context, the G_{Ico} value defined by Eq. (8) is taken as the mean value, and its standard deviation is assumed to be 10% (i.e., a scatter of $\pm 10\%$). A schematic of the variation of G_{Ic} with respect to crack density as a result of Eqs. 8–10 is shown by the data points plotted in Fig. 2b.

2.3. Overall modeling procedure

The complete procedure for predicting micro-crack initiation and propagation in multiple plies of a general symmetric laminate is outlined in Fig. 3. The multiaxial quasi-static load applied to the laminate is incremental strain-controlled loading. The following input data is required for the MATLAB routine: (i) the lamina engineering constants E_1, E_2, G_{12} , and ν_{12} , (ii) the undamaged laminate engineering constants E_x, E_y, G_{xy} , and ν_{xy} evaluating using classical laminate theory (CLT), (iii) the normalized COD (and CSD) values and the corresponding damage constants $a_i^{(\alpha)}$ evaluated from micromechanical FE analysis [23], (iv) the numerically computed G_{Ico} (and G_{IIco}) values for each ply, (v) the corresponding Weibull

parameters G_0 and m , and (vi) the applied laminate strain increments $\Delta\epsilon_x, \Delta\epsilon_y$, and $\Delta\gamma_{xy}$. The main strain loop controls the applied laminate strain based on the specified multiaxial strain increments. Iterations are performed during each applied strain level, and for each ply, to determine the current crack densities using a virtual crack technique as shown in Fig. 3. The specified segments along the length of each ply are randomly analyzed to determine whether a new crack will initiate during the current applied strain level. Equations (5), (8)–(10) are used to evaluate the crack multiplication criterion specified by Eq. (7), and the iteration continues during a certain strain level so long as the criterion holds true. Once the criterion is not met, cracking in the relevant ply will not continue during that particular strain level. This process is repeated for each ply in the laminate, and continually repeated as the applied strain levels are incremented. During each strain increment the updated laminate stiffness tensor $C_{ijkl}(\rho_\alpha)$ and stress components σ_{ij} are evaluated, and the routine stores the current laminate stresses and strains, ply crack densities, and laminate engineering constants. The process is repeated until the specified stop criteria is met, which is when a critical strain level or a critical stiffness value is attained. This methodology is able to predict simultaneous evolution of multiple ply cracks, while accounting for

Table 1
Lamina properties.

Lamina	E_1 (GPa)	E_2 (GPa)	G_{12} (GPa)	ν_{12}	t_{ply} (mm)
T300/934	144.8	11.38	6.48	0.30	0.132
E-glass/Epikote	46	13	5	0.30	0.50

Table 2
Computed lamina initial critical strain energy release rates and Weibull parameters.

Lamina	90° ply			0° ply		
	G_{Ico} (J/m ²)	G_o (J/m ²)	m	G_{Ico} (J/m ²)	G_o (J/m ²)	m
[0/90] _s CFRP	171.1	179	12.19	204.7	213	12.15
[0/90 ₂] _s CFRP	173.5	181	12.15	204.9	214	12.16
[0/90] _s GFRP	274.7	286	12.13	319.6	333	12.14
[0/90 ₂] _s GFRP	345.2	360	12.15	322.9	337	12.16

crack interactions between adjacent cracked plies though the normalized COD (and CSD) functions [23].

3. Results

In order to showcase the predictive capabilities of the improved damage evolution model, four cross-ply laminates are analyzed here according to the availability of experimental crack density evolution data [5, 13]. Again, it should be noted that all experimental data presented in this study was obtained from previously reported experimental studies from the literature. These include two laminate stacking sequences of [0/90]_s and [0/90₂]_s, with glass fiber/epoxy and carbon fiber/epoxy material systems. The in-plane lamina properties for the GFRP and CFRP laminates are provided in Table 1. The corresponding G_{Ico} values determined using the 3D micromechanical FE approach described in Section 2.2, and the corresponding Weibull distribution parameters for the four

laminates are presented in Table 2. In previous models, G_{Ico} was obtained by fitting the damage evolution model to the experimental data for a chosen reference laminate [19, 21]. The FE approach presented here not only takes out this empiricism from the model, but also eliminates need to select a reference laminate and conduct expensive and time-consuming experimental testing. It is the authors' belief that this would also decrease inaccuracies inherent in the previous model where the same G_{Ico} was used for different ply orientations. From Table 2 it is clear that G_{Ico} increases with increasing 90° ply thickness, which is consistent with previous studies [35, 40]. Nonetheless, laminates containing thicker plies will have lower ply crack initiation strains since larger COD values lead to increased strain energy. As expected, the G_{Ico} values for the CFRP laminates are greater than those of the GFRP laminates, and would correspond to higher crack initiation strains. For all cross-ply laminates studied here, the Weibull shape parameter m was found to be approximately 12.1, assuming a standard deviation of 10% in G_{Ic} (see Eq. (8)). The shape parameter is consistent for the carbon-fiber and glass-fiber laminates considered in this study, but it should be noted that the parameter may change for other material systems (e.g., kevlar/epoxy).

The results of the crack evolution predictions for the laminates subjected to uniaxial loading are shown in Fig. 4 as 90° ply crack density plotted against axial applied stress. The model predictions seem to correlate well with available experimental data for all four laminate types. When G_{Ic} is considered independent of crack density (Fig. 4a, c), the crack densities are over-predicted, which demonstrates the need to consider the increasing resistance to ply micro-cracking with crack density evolution (Eq. (9)). Furthermore, the CFRP laminates (Fig. 4a, b) have a greater resistance to ply cracking compared to the GFRP laminates (Fig. 4c, d), and thus can handle greater axial loads before ply cracking ensues. The ability of the developed model to predict lower crack initiation stresses for laminates with greater 90° ply thickness is seen by comparing Fig. 4a and b, and Fig. 4c and d. This result is attributed to the

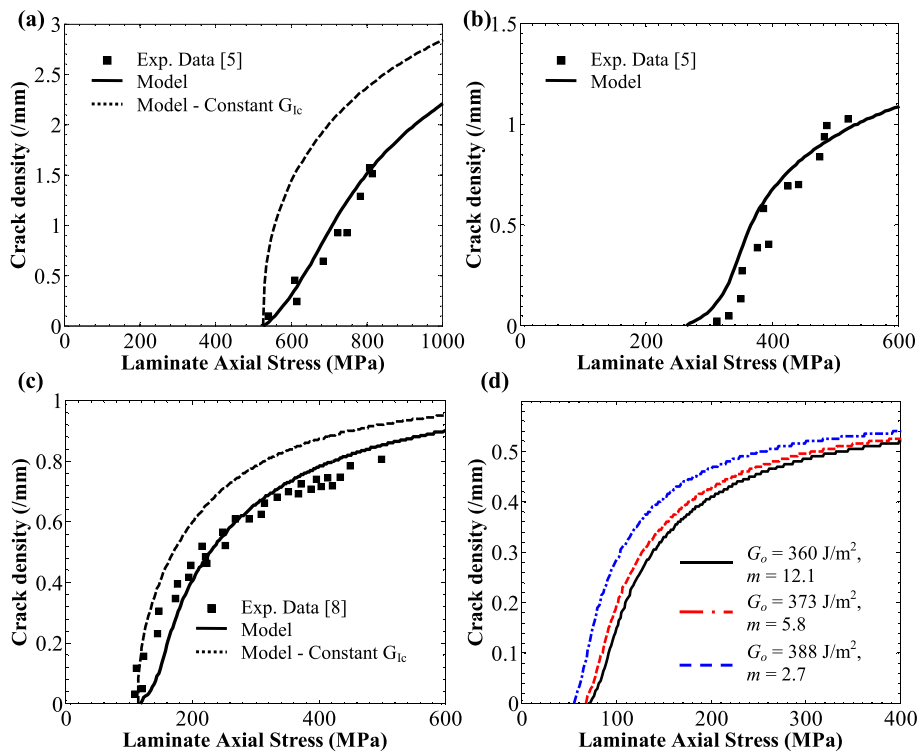


Fig. 4. 90° ply crack density evolution in (a) [0/90]_s CFRP, (b) [0/90₂]_s CFRP, (c) [0/90]_s GFRP, and (d) [0/90₂]_s GFRP laminates.

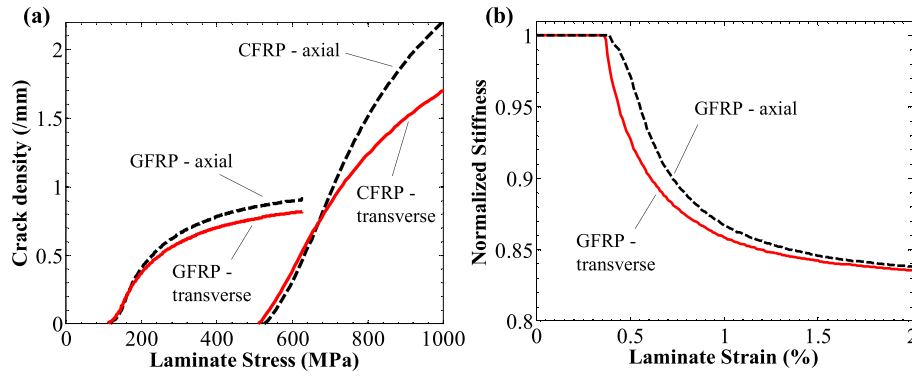


Fig. 5. Longitudinal and transverse uniaxially loaded $[0/90]_s$ laminates (a) crack density evolution plots, (b) stiffness degradation plots for GFRP.

energy-based approach, and is consistent with a number of other studies on cross-ply laminates [4, 7, 35, 40]. The effect of changing the Weibull parameters, G_0 and m , on the evolving crack density for the $[0/90]_s$ GFRP laminate is demonstrated in Fig. 4d. A variation of the standard deviation of G_{IC0} between 10% and 40%, resulting in the indicated G_0 and m values, has a direct influence on crack initiation strain, which varies by up to 20%. Also, the crack densities at higher applied stresses for the data shown in Fig. 4d have a 15% scatter. Similar observations were reported by Berthelot and LeCorre [42], where a larger scatter of the laminate strength data shifted the crack density curves to the left, resulting in lower crack initiation stresses.

The results of crack evolution predictions for the $[0/90]_s$ laminates subjected to uniaxial loading in either the longitudinal or transverse directions are shown in Fig. 5. In this case transverse uniaxial loading is equivalent to longitudinal uniaxial loading of a $[90/0]_s$ laminate, whereby the cracked plies are on the laminate surface (i.e., outer plies). The model clearly predicts earlier onset of cracking for the transversely loaded CFRP and GFRP laminates when compared to the same laminates loaded longitudinally (Fig. 5a). When cracked plies are on the surface of the laminate, they are expected to crack earlier since they are only constrained on one side, whereas when a cracked ply is within the laminate the additional constraining effect delays the onset of cracking. The model also predicts a greater degree of stiffness degradation for the transversely loaded laminates (Fig. 5b), which is a result of increased COD for the laminate with cracked outer plies. In addition, although crack initiation occurs at higher loads for the longitudinally loaded laminates, their crack density is greater at higher loads. These trends are

consistent with previous experimental observations for similar cross-ply laminates [43].

Damage evolution predictions for the $[0/90]_s$ CFRP cross-ply laminate subjected to equibiaxial loading in the longitudinal and transverse directions are shown in Fig. 6, which also includes the corresponding stress-strain curves predicted using Eqs. (1)–(3). In this case, cracks in the thicker 90° ply initiated prior to cracks in the outer 0° ply as shown in Fig. 6a, which is expected. The 90° ply cracks initiated at an applied strain of 0.37%, which is less than that of the uniaxial case where cracks initiated at 0.48% applied strain (see Fig. 4b). This is attributed to the added applied transverse strain, and follows predictions by other researchers [6]. The effects of damage evolution on the nonlinear axial and transverse stress-strain behaviour has been clearly captured as shown in Fig. 6b. The corresponding normalized material property degradation curves for biaxial loading are presented in Fig. 7a. The axial modulus, E_x , begins to degrade when the 90° ply cracks initiate, whereas the transverse modulus, E_y , begins to degrade when the 0° ply cracks initiate. The in-plane shear modulus, G_{xy} , and Poisson's ratio, ν_{xy} , also begin to degrade at 0.37% strain, but exhibit enhanced degradation at 0.50% due to the addition of 0° ply cracks. This is due to the reduction in shear deformation resistance caused by the addition of these splitting cracks, demonstrating the combined effect of the two damage modes on the material properties. Similar material property degradation behaviour was found for other cross-ply laminates analyzed in this study. A comparison of the normalized G_{xy} and ν_{xy} degradation curves in Fig. 7a and b for equibiaxial and uniaxial loading at the indicated applied strain of 0.75%, which corresponds to crack densities of 1 cr/mm in each of the 90° and 0° plies, demonstrates that the addition of splitting

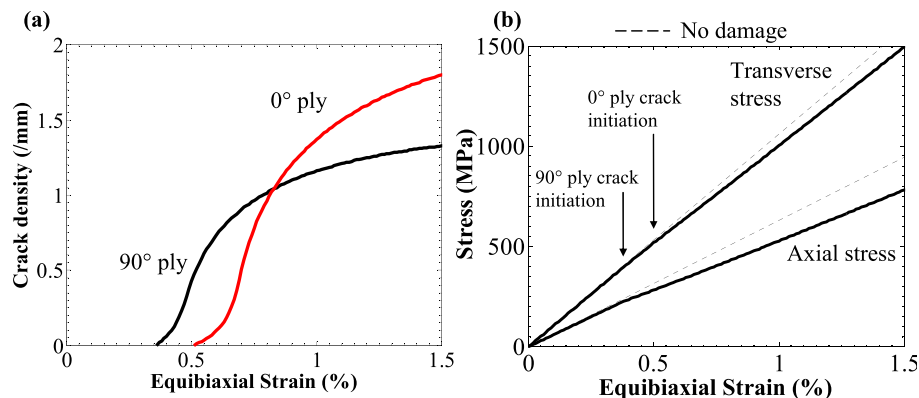


Fig. 6. Equibiaxial loaded $[0/90]_s$ CFRP laminate (a) crack density plots, (b) stress–strain data.

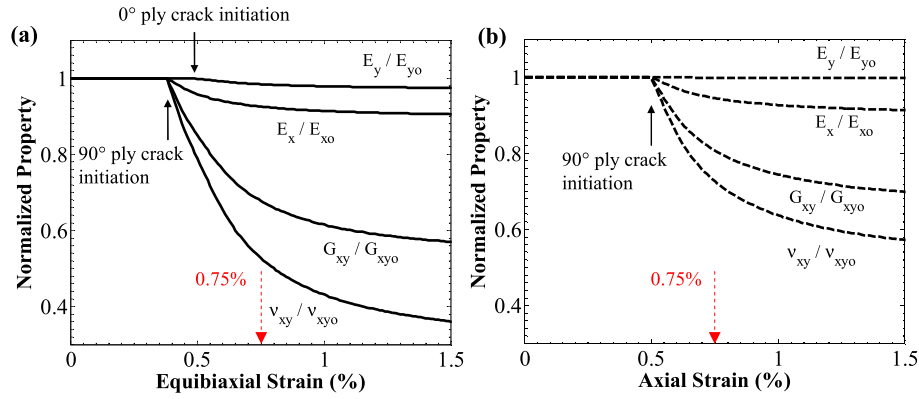


Fig. 7. Normalized material property degradation plots for $[0/90]_s$ CFRP laminate subjected to (a) equibiaxial loading, (b) uniaxial loading.

cracks enhanced the degradation of G_{xy} and ν_{xy} by 20% and 15% respectively. Kashtalyan and Soutis [44] used a shear-lag model for a similar GFRP cross-ply laminate containing the same crack density, and reported a 15% enhanced reduction for both G_{xy} and ν_{xy} when axial splits were considered, which is comparable to the predictions of the model presented here. It should be noted that the shear lag model [44] did not predict damage evolution, and to the knowledge of the authors, experimental or predicted crack density evolution data for cross-ply laminates loaded biaxially are not available in the literature.

The developed model was also used to predict the laminate crack evolution behaviour for various applied biaxial loading ratios (i.e., ϵ_x/ϵ_y). One of the key findings for these predictions was the variation of crack initiation stress with the applied biaxial loading ratio. Fig. 8a and b presents the predicted crack initiation envelopes for the indicated CFRP and GFRP cross-ply laminates, respectively, where crack initiation corresponds to cracks initiating in either the

0° or 90° plies. It is clear that the addition of a transverse stress (strain) component slightly decreases the laminate axial stress at which 90° ply cracks initiate, which is due to the added laminate out-of-plane contraction caused by Poisson's effect [23], which results in more strain energy being added to the laminate. A similar trend was found with the splitting cracks in the 0° plies, resulting in the distinct shape of the damage initiation envelopes shown in Fig. 8. The approximate 'square' shape of the envelopes presented in Fig. 8 is consistent with predicted and experimental biaxial crack initiation envelopes reported in Refs. [45–47], and seems to be characteristic of cross-ply laminates. It should be noted that the biaxial crack initiation envelope of a laminate does not necessarily have the same shape as its final failure envelope as was reported by Sun and Tao [46]. It is also notable that the $[0/90]_s$ laminate crack initiation envelopes are not symmetric about the diagonal lines drawn in the plots of Fig. 8a and b, which is due to the difference in crack initiation strains of the outer 0° plies in comparison to the

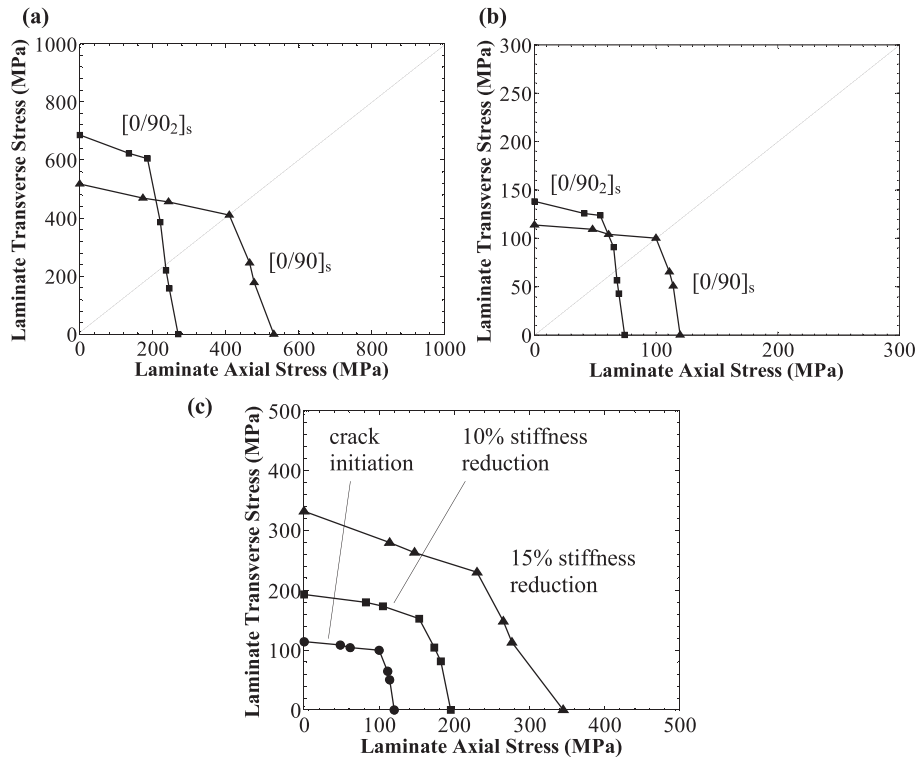


Fig. 8. Biaxial crack initiation envelopes for (a) CFRP laminates, (b) GFRP laminates; (c) $[0/90]_s$ GFRP laminate biaxial critical stiffness degradation envelopes.

inner 90° plies. Corresponding crack evolution plots for the $[0/90]_s$ CFRP and $[0/90_2]_s$ GFRP laminates are shown in Fig. 9, further illustrating the influence of biaxial loading ratio on 90° ply crack initiation strain. For the $[0/90]_s$ CFRP laminate the uniaxial crack initiation strain is 0.65%, decreasing to 0.48% for the equibiaxial prediction, whereas for the $[0/90_2]_s$ GFRP laminate, the strain reduces from 0.31% to 0.22% for the same predictions. For all laminates, the crack density evolution also increased as a result of biaxial loading, as is depicted in Fig. 9.

The predicted crack initiation envelope for the $[0/90]_s$ GFRP laminate is re-plotted in Fig. 8c along with 10% and 15% stiffness degradation envelopes, which correspond to degradation of either the axial stiffness, E_x , or transverse stiffness, E_y . The stiffness degradation envelopes are similar in shape to the crack initiation envelope, and they provide critical design criteria that is important for stiffness-based designs, showcasing the applicability of the presented prediction model for practical problems. The relative position of the stiffness degradation envelopes in Fig. 8c illustrates the ability of the model to predict the characteristic nonlinear stiffness degradation behaviour of the cross-ply laminates.

4. Discussion

Although the model's capabilities have been clearly shown, there are some limitations worth mentioning as the model development continues. Firstly, the current model is capable of accounting for mode II CSD when predicting damage evolution (see Eq. (6)), which can be evaluated using micromechanical FE analysis [23]. However, the CSDs are neglected for stiffness tensor evaluation defined by Eq. (2). It is not clear at this stage whether or not the addition of CSDs will greatly influence the stiffness predictions for general multidirectional laminates. Preliminary evaluations using micromechanical FE models suggest that the effect on axial and transverse stiffness degradation is minimal, whereas the influence of CSDs on shear modulus is more notable. Additional investigations are required and may result in reformulation of the constraint parameter κ_α in Eq. (1), however this is left for a future study. Secondly, the model currently utilizes an analytical expression in Eq. (9) to evaluate the variation of G_{Ic} with crack density, which is suitable for cross-ply laminates. The applicability of this expression for multidirectional laminates is not clearly known at this stage. It is believed that the same expression will be applicable for carbon fiber/polymer and glass fiber/polymer multidirectional laminates since the crack multiplication criteria would be similar for plies of different orientations. In addition, the scope of the prediction model is limited to the evolution of sub-critical intra-ply matrix cracks, and the corresponding material property

degradation. Thus, the model is capable of predicting stiffness degradation prior to the onset of critical damage modes, which is suitable for predicting the durability of many practical composite structures (see Fig. 8c). If the current model is adopted for predicting failure in the sense that there is a total loss of load-bearing capacity, then critical damage modes such as delamination and fiber fracture must also be considered and coupled with a suitable failure criteria. This is important for predicting the durability of composite structures, and generally for designing fail-safe structures. Regarding the effects of delamination on the laminate response, this can be directly accounted for by the three dimensional micromechanical FE model. Regarding fiber fracture, a suitable fiber failure criterion can be incorporated in the prediction model. This is however left for a future study. Finally, compressive damage modes are currently not considered by the model, and would have to be investigated before being invoked for predicting crack evolution of composite structures subjected to high magnitude compressive loading.

5. Conclusions

This paper presented the development of an energy-based multiscale damage evolution prediction model for symmetric laminates containing sub-critical matrix cracks in multiple orientations, and subjected to multiaxial loading. The model utilized computational micromechanics, in lieu of experimental data, to define ply level matrix crack critical strain energy release rates as well as the laminate material damage constants, which is an advantage when compared to existing models reported in the literature. An analytical expression was also utilized to capture the increased resistance to ply cracking with increasing ply crack density. Moreover, a Weibull distribution was utilized for the critical strain energy release rates in order to account for the stochastic nature of matrix crack evolution. The effect of crack interactions at higher matrix crack densities (i.e., crack shielding) was also accounted for through the use of continuous sigmoidal functions representing the crack opening displacements. The model also accounts for the effects of applied multiaxial strains on crack evolution and material property degradation, which is a key contribution.

The crack evolution predictions for several cross-ply laminates subjected to uniaxial and multiaxial strains have demonstrated the model's capabilities. These include predicting crack evolution in both CFRP and GFRP laminates, and accounting for the influence of ply thickness and laminate stacking sequence on crack initiation and evolution, which can be attributed to the energy-based approach used. In addition, crack initiation envelopes and critical

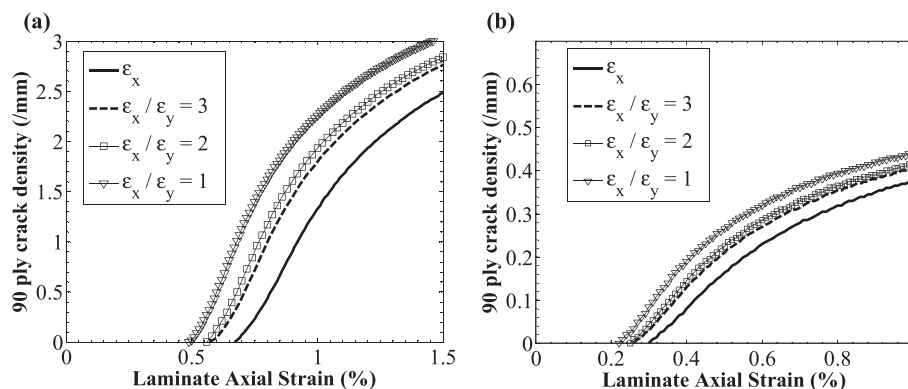


Fig. 9. Laminate biaxial loading crack density evolution (a) $[0/90]_s$ CFRP, (b) $[0/90_2]_s$ GFRP.

stiffness degradation envelopes were predicted for the laminates considered. It is also worth noting that the developed multiscale prediction scheme is suitable for implementation into displacement-based finite element software packages, such as ANSYS or ABAQUS, in order to predict damage evolution and stiffness degradation of composite structures. This will ultimately provide a means to predict the durability and structural integrity of primary load bearing composite structures.

Acknowledgements

The authors would like to thank the Natural Sciences and Engineering Research Council (NSERC) of Canada, and the University of Toronto for funding in support of this work.

References

- [1] Highsmith AL, Reifsnider K. Stiffness-reduction mechanisms in composite laminates. In: Reifsnider K, editor. *Damage in composite materials*. Philadelphia: ASTM STP 775; 1982. p. 103–17.
- [2] Hashin Z. Analysis of cracked laminates: a variational approach. *Mech Mater* 1985;4:121–36.
- [3] Talreja R. Transverse cracking and stiffness reduction in composite laminates. *J Compos Mater* 1985;19:355–75.
- [4] Liu S, Nairn JA. The formation and propagation of matrix microcracks in cross-ply laminates during static loading. *J Reinf Plast Compos* 1992;11:158–78.
- [5] Zhang J, Fan J, Soutis C. Analysis of multiple matrix cracking in $[\pm\theta_m/90_n]_s$ composite laminates - part 2: development of transverse ply cracks. *Composites* 1992;23:299–304.
- [6] McCartney LN. Predicting transverse crack formation in cross-ply laminates. *Compos Sci Technol* 1998;58:1069–81.
- [7] Joffe R, Krasnikovs A, Varna J. COD-based simulation of transverse cracking and stiffness reduction in $[S/90_n]_s$ laminates. *Compos Sci Technol* 2001;61:637–56.
- [8] Lundmark P, Varna J. Crack face sliding effect on stiffness of laminates with ply cracks. *Compos Sci Technol* 2006;66:1444–54.
- [9] Barbero EJ, Cosso FA. Determination of material parameters for discrete damage mechanics analysis of carbon-epoxy laminates. *Compos Part B* 2014;56:638–46.
- [10] Berthelot JM. Transverse cracking and delamination in cross-ply glass-fiber and carbon-fiber reinforced plastic laminates: static and fatigue loading. *Appl Mech Rev* 2003;56:111–47.
- [11] Masters J, Reifsnider K. An investigation of cumulative damage development in quasi-isotropic graphite/epoxy laminates. In: Reifsnider K, editor. *Damage in composite materials*. Philadelphia: ASTM STP 775; 1982. p. 40–62.
- [12] Gudmundson P, Zang W. An analytic model for thermoelastic properties of composite laminates containing transverse matrix cracks. *Int J Solids Struct* 1993;30:3211–31.
- [13] Tong J, Guild FJ, Ogin SL, Smith PA. On matrix crack growth in quasi-isotropic laminates - I. experimental investigation. *Compos Sci Technol* 1997;57:1527–35.
- [14] Varna J, Joffe R, Akshantala VN, Talreja R. Damage in composite laminates with off-axis plies. *Compos Sci Technol* 1999;59:2139–47.
- [15] Yokozeki T, Aoki T. Overall thermoelastic properties of symmetric laminates containing obliquely crossed matrix cracks. *Compos Sci Technol* 2005;65:1647–54.
- [16] Kashtalyan M, Soutis C. Stiffness and fracture analysis of laminated composites with off-axis ply matrix cracking. *Compos Part A* 2007;38:1262–9.
- [17] Varna J. Physical interpretation of parameters in synergistic continuum damage mechanics model for laminates. *Compos Sci Technol* 2008;68:2592–600.
- [18] Singh CV, Talreja R. A synergistic damage mechanics approach for composite laminates with matrix cracks in multiple orientations. *Mech Mater* 2009;41:954–68.
- [19] Singh CV, Talreja R. Evolution of ply cracks in multidirectional composite laminates. *Int J Solids Struct* 2010;47:1338–49.
- [20] Barbero EJ, Cortes DH. A mechanistic model for transverse damage initiation, evolution, and stiffness reduction in laminated composites. *Compos Part B* 2010;41:124–32.
- [21] Singh CV, Talreja R. A synergistic damage mechanics approach to mechanical response of composite laminates with ply cracks. *J Compos Mater* 2013;47:2475–501.
- [22] Huang Y, Talreja R. Statistical analysis of oblique crack evolution in composite laminates. *Compos Part B* 2014;65:34–9.
- [23] Montesano J, Singh CV. A synergistic damage mechanics based multiscale model for composite laminates subjected to multiaxial strains. *Mech Mater* 2015;83:72–89. <http://dx.doi.org/10.1016/j.mechmat.2015.01.005>.
- [24] Daniel IM, Tsai CL. Analytical/experimental study of cracking in composite laminates under biaxial loading. *Compos Eng* 1991;1:355–62.
- [25] Welsh JS, Mayes JS, Biskner AC. 2-D biaxial testing and failure predictions of IM7/977-2 carbon/epoxy quasi-isotropic laminates. *Compos Struct* 2006;75:60–6.
- [26] Schuecker C, Pettermann HE. A continuum damage model for fiber reinforced laminates based on ply failure mechanisms. *Compos Struct* 2006;76:162–73.
- [27] Mayugo JA, Camanho PP, Maimi P, Davila CG. Analytical modelling of transverse matrix cracking of $[\pm\theta/90^0]_s$ composite laminates under multiaxial loading. *Mech Adv Mater Struct* 2010;17:237–45.
- [28] Vyas GM, Pinho ST. Computational implementation of a novel constitutive model for multidirectional composites. *Comp Mater Sci* 2012;51:217–24.
- [29] Laurin F, Carrere N, Huchette C, Maire JF. A multiscale hybrid approach for damage and final failure predictions of composite structures. *J Compos Mater* 2013;47:2713–47.
- [30] Chamis CC, Abdi F, Garg M, Minnetyan L, Baid H, Huang D, et al. Micro-mechanics-based progressive failure of analysis prediction for WWFE-III composite coupon test cases. *J Compos Mater* 2013;47:2695–712.
- [31] Kashtalyan M, Soutis C. Predicting residual stiffness of cracked composite laminates subjected to multi-axial inplane loading. *J Compos Mater* 2013;47:2513–24.
- [32] Varna J. Modelling mechanical performance of damaged laminates. *J Compos Mater* 2013;47:2443–74.
- [33] Talreja R. Damage characterization by internal variables. In: Talreja R, editor. *Damage mechanics of composite materials*. Amsterdam: Elsevier; 1994. p. 53–78.
- [34] Irwin G. *Handbuch der Physik VI* (Chapter: fracture I). Berlin: Springer; 1958. p. 551–90.
- [35] Han YM, Hahn HT. A simplified analysis of transverse ply cracking in cross-ply laminates. *Compos Sci Technol* 1988;31:165–77.
- [36] Rybicki EF, Kanninen MF. A finite element calculation of stress intensity factors by a modified crack closure integral. *Eng Fract Mech* 1977;9:931–8.
- [37] Buchholz FG, Rikards R, Wang H. Computational analysis of interlaminar fracture of laminated composites. *Int J Fract* 1997;86:37–57.
- [38] Yokozeki T, Aoki T, Ishikawa T. Consecutive matrix cracking in contiguous plies of composite laminates. *Int J Solids Struct* 2005;42:2785–802.
- [39] Rebiere JL, Gamby D. Strain energy release rate analysis of matrix micro cracking in composite cross-ply laminates. *Mater Sci App* 2011;2:537–45.
- [40] Vinogradov V, Hashin Z. Probabilistic energy based model for prediction of transverse cracking in cross-ply laminates. *Int J Solids Struct* 2005;42:365–92.
- [41] Wang F, Zhang J, Li L, Chen Z. ECM-based statistical simulation of progressive failure in symmetric laminates damaged by transverse ply cracking. In: *Proceedings of the 13th international conference on fracture*. Beijing, China; June 16–21, 2013.
- [42] Berthelot JM, LeCorre JF. Statistical analysis of the progression of transverse cracking and delamination in cross-ply laminates. *Compos Sci Technol* 2000;60:2659–69.
- [43] Nairn JA, Hu S. The formation and effect of outer-ply microcracks in cross-ply laminates: a variational approach. *Eng Fract Mech* 1992;41:203–21.
- [44] Kashtalyan M, Soutis C. Stiffness degradation in cross-ply laminates damaged by transverse cracking and splitting. *Compos Part A* 2000;31:335–51.
- [45] Wurzel DP. On the design and optimization of bidirectional composites. *J Reinf Plast Compos* 1983;2:178–95.
- [46] Sun CT, Tao J. Prediction of failure envelopes and stress/strain behaviour of composite laminates. *Compos Sci Technol* 1998;58:1125–36.
- [47] Welsh JS, Mayes JS, Key CT, McLaughlin RN. Comparisons of MCT failure prediction techniques and experimental verification for biaxially loaded glass fabric-reinforced composite laminates. *J Compos Mater* 2004;38:2165–81.